Polymer Chemistry

Accepted Manuscript

ROYAL SOCIETY OF CHEMISTRY

www.rsc.org/polymers

Graphical Abstract

Chiroptical and emissive properties of a calix[4]arene-containing chiral poly(*p*-phenyleneethynylene) with enantioselective recognition ability

José V. Prata,[a]*Alexandra I. Costa,[a] Gennaro Pescitelli[b] and Hugo D. Pinto[a]

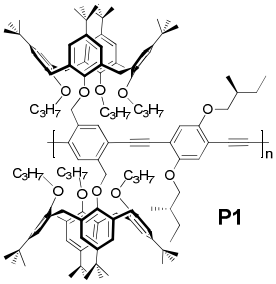

Non-aggregated state:
× CD-silent
× No binding capacity

Aggregated state:
✓ CD-active
✓ Enantioselective host for chiral amines

*Corresponding author. E-mail: jvprata@deq.isel.ipl.pt;
Phone: (+) 351-218317172; Fax: (+) 351-218317267.

Chiroptical and emissive properties of a calix[4]arene-containing chiral poly(*p*-phenyleneethynylene) with enantioselective recognition ability

José V. Prata,[a*] Alexandra I. Costa,[a] Gennaro Pescitelli[b] and Hugo D. Pinto[a]

[a]*Laboratório de Química Orgânica, Departamento de Engenharia Química and Centro de Investigação de Engenharia Química e Biotecnologia, Instituto Superior de Engenharia de Lisboa, Instituto Politécnico de Lisboa, R. Conselheiro Emídio Navarro, 1, 1959-007, Lisboa, Portugal;* [b]*Dipartimento di Chimica e Chimica Industriale, Università di Pisa, via Risorgimento, 35, 56126 Pisa, Italy*

[*]*Corresponding author.* E-mail: jvprata@deq.isel.ipl.pt;
Phone: (+) 351-218317172; Fax: (+) 351-218317267.

Abstract

Supramolecular chirality was achieved in solutions and thin films of a calixarene-containing chiral aryleneethynylene copolymer. The observed chiroptical activity, which is primarily allied with the formation of aggregates of high molecular weight polymer chains, is a result of a combination of intrachain and interchain effects. The former arise by the adoption of an induced helix-sense by the polymer main-chain while the later come from the exciton coupling of the aromatic backbone transitions. The co-existence of bulky bis-calix[4]arene units and chiral side-chains on the polymer skeleton prevents efficient π-stacking of neighbouring chains, keeping the chiral assembly highly emissive. In contrast, for a model polymer lacking calixarene moieties, the chiroptical activity is dominated by strong interchain exciton couplings as a result of more favourable packing of polymer chains, leading to a marked decrease of photoluminescence for the aggregate state. The enantiomeric recognition abilities of both polymers toward (*R*)- and (*S*)-α-methylbenzylamine were examined. It was found that a significant enantiodiscrimination is exhibited by the calixarene-based polymer.

Introduction

The study of chemistry, optical properties and applications of oligomeric[1] and polymeric[2] *p*-phenyleneethynylenes (*p*-PEs) has steadily grown over the past two decades. Poly(*p*-PE)s (PPEs) are, amongst conjugated macromolecules, one of the classes exhibiting the most intense fluorescence efficiencies in solution and as films.[3] This property, in addition to their photo and chemical stability, makes them particularly useful as sensory materials for chemical and biological species.[2b] Sensing systems based on fluorescence optical transduction methods are in general highly sensitive.[4] PPEs, in particular, have long been established as tremendously effective optical sensors.[5]

Incorporation of suitable molecular receptors into aryleneethynylene polymer frameworks may potentiate specific supramolecular host-guest interactions and lead to enhanced sensory responses. In particular, taking advantage of the rich chemistry and the well-known molecular recognition capabilities of calix[4]arenes,[6] several poly(aryleneethynylene)s (PAEs) containing calixarene receptors have been prepared by us[7] and others,[8] and applied as sensors toward various classes of molecules.[8,9]

In addition to providing well-defined recognition sites, calix[4]arene units may efficiently prevent a strong stacking between polymer chains by creating a wrap over the PAE molecular wire.[7a,7c] It is well known that interchain interactions of polymer chains in fluid aggregated phases and in films strongly influence and govern the optoelectronic properties of the resultant supramolecular assemblies and of materials obtained thereby.[10] Too strong interchain interactions may lead to poor fluorescent materials (either by self-quenching and/or formation of excimer-like species) and reduced exciton diffusion along a polymer chain.[11] Two strategies have been successfully employed to hamper strong interchain interactions in conjugated polymers. One is the introduction of bulky side-chain groups or scaffolds, such as calix[4]arenes or pentiptycenes, which provide a sort of insulator along the chains.[7a,12] A

second, more recent, strategy consists of attaching stereodefinite chiral moieties to PPE backbones, either of biological[13] or synthetic origin.[14] The introduction of chirality forces the chains to adopt a twisted mutual arrangement and discourages a perfect alignment.[11,15] Moreover, optically active materials may be characterized by chiroptical spectroscopies such as electronic circular dichroism, which offers many advantages in the investigation of supramolecular species.[16] Additionally, chiral materials may be employed to build enantioselective sensors with potential applications in the field of chiral recognition of (bio)molecular species.[17]

Within this framework, we became interested in exploring the properties of calixarene-containing chiral aryleneethynylene copolymers. This kind of PPEs combines the two elements of bulkiness and chirality described above, and provides additional sites for molecular recognition. We report herein the synthesis, photophysical and chiroptical properties of a new *p*-phenyleneethynylene *alt*-copolymer (**P1**) bearing a calix[4]arene and a homochiral alkylated side-chain as alternating elements (Figure 1). For comparison, a model polymer (**P2**) lacking calixarene units was also investigated.

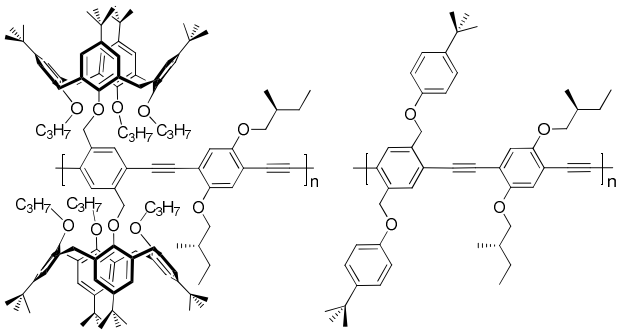

Figure 1. Chiral-substituted poly(*p*-phenyleneethynylene) copolymers used in the study.

The main focus of our study is the mechanism of induction of supramolecular chirality in this type of polymers, namely, how chiral information is transferred from the molecular to the supramolecular scale. In addition, preliminary studies concerning the enantioselective binding

of both polymers toward optically active amines [(*R*)- and (*S*)-α-methylbenzylamine] are also described, as a proof of concept of the potential sensory applications of the calix[4]arene-based polymer.

Experimental section

Instruments and methods. Infrared spectra (FT-IR) were measured on a Bruker Vertex 70 as films (transmission mode). ^{1}H NMR and ^{13}C NMR spectra were collected on a Bruker AVANCE II^{+} spectrometer (400 MHz) at 25ºC; reported chemical shifts (δ/ppm) are internally referenced to TMS. The splitting parameters for ^{1}H NMR are denoted as follows: s (singlet) and m (multiplet). ^{1}H-^{1}H Correlation Spectroscopy (COSY), ^{13}C-^{1}H Heteronuclear Single Quantum Correlation (HSQC), Heteronuclear Multiple Bond Correlation (HMBC) and Nuclear Overhauser Effect Spectroscopy (NOESY) NMR techniques were used for spectral assignments. Elemental analyses were performed at the Laboratorio Análisis Instrumental (C.A.C.T.I.) of Universidad de Vigo. Gel permeation chromatography (GPC) analysis was performed on a Jasco Liquid Chromatography system equipped with a Jasco PU-2089 Plus Pump, a Jasco CO-2065 Plus Column Oven and a Jasco UV-1575 UV-Vis Detector (monitoring at 270 nm), using PSS SDV columns (10^3 and 10^5 Å) and THF as eluent at 35ºC. Calibration was done with monodisperse polystyrene standards. The polymeric/oligomeric contents of the polymerization mixtures, the degrees of conversion, and the final composition of the isolated materials, as well as the number-average (M_n) and weight-average (M_w) molecular weights were estimated from the GPC traces based on UV response. The polymerization yields were determined gravimetrically. Polymer concentrations are based on the molecular weight of the repeat unit, and so expressed everywhere in the text. Electronic circular dichroism (CD) and UV-Vis spectra were recorded simultaneously on a JASCO J-815 CD spectrometer either in solution (at 2.0 x 10^{-5} M in $CHCl_3$ and $CHCl_3$:MeOH mixtures, unless stated otherwise) or as thin films, using 1-cm quartz cells at 20ºC. For CD and

absorption variable temperature measurements, temperature control was achieved with a Jasco Peltier type accessory CDF-426S/426L. Absorption titration experiments with optically active amines were conducted on a Nicolet Evolution 300 spectrophotometer using 1-cm quartz cells at 25ºC. Steady-state fluorescence spectra were recorded on a Perkin Elmer LS45 fluorimeter using a 1-cm quartz cuvette in right angle (RA) or front-face (FF; oriented at *ca*. 30º relative to the incident beam) geometries at 25ºC. Fluorescence quantum yields in solution were measured using 9,10-diphenylanthracene (9,10-DPA) as reference (Φ= 0.95 in ethanol)[18] at 25ºC. To prevent inner filter effects during quantum yield measurements the optical density (OD) of the samples and reference were kept below 0.05 at the excitation wavelength (380 nm); solutions of the polymers were prepared in chloroform while that of 9,10-DPA in ethanol. Fluorescence spectra were recorded under the same operating settings. Quantum yields were determined using the equation $\Phi = \Phi_r \times I/I_r \times OD_r/OD \times n^2/n^2_r$,[19] where Φ is the quantum yield, I is the integral of fluorescence emission intensity, OD denote the optical density at the specified wavelength, with the subscript r referring to the reference; n and n_r are the refractive indices of $CHCl_3$ and EtOH, respectively.

Materials. 1,4-Bis-[5,11,17,23-tetrakis(1,1-dimethylethyl)-25-(oxymethyl)-26,27,28-tripropyloxycalix[4]arene]-2,5-diiodobenzene (**1**; diiodo-biscalix[4]arene) and 1,4-bis-(*p-tert*-butylphenoxymethyl)-2,5-diiodo-benzene (**2**; diiodo-TBP), were prepared according to our reported procedures,[7a] and fully characterized by FT-IR, $^1H/^{13}C$ NMR and microanalysis. 2,5-Diiodo-1,4-hydroquinone was prepared by a literature procedure.[20] Dichlorobis(triphenylphosphine)palladium (II) (98%, Aldrich), copper(I) iodide (98%, Aldrich), 9,10-diphenylanthracene (scintillation grade, Nuclear Enterprises), (*R*)-α-methylbenzylamine (98%, Fluka), and (*S*)-α-methylbenzylamine (98%, Alfa Aesar) were used as received. Triethylamine (99%, Riedel-de-Haën) was previous dried from CaH_2 and distilled under N_2 prior to use; toluene was previous dried from Na, distilled under N_2 and stored over Na. Other

reagents and solvents were reagent grade and were purified and dried by standard methods. Organic extracts were dried over anhydrous magnesium sulphate.

Synthesis. Poly((2,5-bis-[5,11,17,23-tetrakis(1,1-dimethylethyl)-25-(oxymethyl)-26,27,28-tripropyloxycalix[4]arene]-*p*-phenylene)ethynylene-*alt*-(2,5-bis-2-(*S*)-methylbutoxy-*p*-phenylene)ethynylene (**P1**). To an argon degassed solution of **1** (50.0 mg, 26.3 μmol) in dry toluene (1.05 mL) and freshly distilled NEt_3 (1.05 mL) was added $PdCl_2(PPh_3)_2$ (1.30 mg, 1.85 μmol) and CuI (0.35 mg, 1.84 μmol) under argon. A degassed solution of **3** (8.62 mg, 28.89 μmol) in dry toluene was then added and the flask sealed. The mixture was stirred in a pre-heated bath at 35ºC, acquiring a fluorescent yellow-greenish colour with turbidity. GPC control after 24h revealed a degree of conversion of ~97% based on **1**. Solvents were removed by evaporation and the residue taken in CH_2Cl_2 and washed successively with 2% aq. HCl, H_2O, aq. $NaHSO_3$ (0.1 M), aq. NH_4SCN (10%), and water. The organic extract was dried and evaporated to dryness. The residue was dissolved in CH_2Cl_2 and poured into MeOH. The precipitate was filtered and dried in a vacuum oven, yielding 64.6% (33.1 mg) of a yellow-greenish solid; FTIR (ν/cm^{-1} (film)): 3040, 2962, 2934, 2875, 2207 (w), 1652, 1602, 1505, 1481, 1466, 1386, 1362, 1300, 1204, 1122, 1041, 1008, 871, 759; UV-Vis (λ_{max}/nm (ε_{max} x 10^{-4} M^{-1}cm^{-1})): 334 (1.983), 434 (4.904); ^{1}H NMR (δ/ppm; $CDCl_3$, 400 MHz): 0.62-0.78 (m, 12H, -$OCH_2CH_2CH_3$, distal rings), 0.83 (s, 18H, -$C(CH_3)_3$), 0.84 (s, 18H, -$C(CH_3)_3$), 0.85-1.10 (m, 18H, -$OCH_2CH_2CH_3$ (6H) and -$OCH_2CH(CH_3)CH_2CH_3$ (12H)), 1.28 (s, 18H, -$C(CH_3)_3$), 1.31 (s, 18H, -$C(CH_3)_3$), 1.23-1.35 (m, 2H, -$OCH_2CH(CH_3)CHHCH_3$, partially overlapped), 1.44-1.66 (m, 2H, -$OCH_2CH(CH_3)CHCH_3$), 1.68-1.78 (m, 2H, -$OCH_2CH(CH_3)CH_2CH_3$), 1.78-1.88 (m, 4H, -$OCH_2CH_2CH_3$), 1.88-2.09 (m, 8H, -$OCH_2CH_2CH_3$, distal rings), 2.94-3.20 (m, 8H, $ArCH_2Ar$ (eq.)), 3.50-3.68 (m, 4H, -$OCH_2CH_2CH_3$), 3.68-3.79 (m, 4H, -$OCH_2CH(CH_3)CH_2CH_3$), 3.79-4.10 (m, 8H, -$OCH_2CH_2CH_3$, distal rings), 4.27-4.46 (m, 4H, ArCHArH (ax.)), 4.46-4.70 (m, 4H, ArCHArH

(ax.)), 4.83-4.93, 4.94-5.17 (m, 4H, $Ar_{calix}OCH_2Ar$), 6.39-6.56 (m, 8H, $Ar_{calix}H$), 6.84-6.96 (m, 2H, $ArH(OC_5H_9)_2$), 6.97-7.11 (m, 8H, $Ar_{calix}H$), 7.73-7.80, 7.90-8.06, 8.25-8.34 (m, 2H, $ArH(CH_2O\text{-Calix})$; *meta-H*-ArI (chain ends), Ar*H* (middle chain) and *ortho-H*-ArI (chain ends), respectively; ratio ~1:6:1); ^{13}C NMR (δ /ppm; $CDCl_3$, 100 MHz): 9.8 ($-OCH_2CH_2CH_3$), 10.7 ($-OCH_2CH(CH_3)CH_2CH_3$), 11.3 (($-OCH_2CH_2CH_3$), 16.5 ($-OCH_2CH(CH_3)CH_2CH_3$), 23.1 ($-OCH_2CH_2CH_3$), 23.4 ($-OCH_2CH_2CH_3$), 26.1 ($-OCH_2CH(CH_3)CH_2CH_3$), 31.2 ($ArCH_2Ar$), 31.2, 31.7 ($ArC(CH_3)_3$), 33.6, 34.0 ($ArC(CH_3)_3$), 34.5 ($-OCH_2CH(CH_3)CH_2CH_3$), 73.8 ($ArOCH_2Ar$), 74.5 ($-OCH_2CH(CH_3)CH_2CH_3$), 76.2, 76.4 ($-OCH_2CH_2CH_3$), 96.2, 96.6 (-C≡C-), 113.8, 121.3 (Ar(*C*)-C≡C-(*C*)Ar), 124.4, 124.5 ($Ar_{calix}(CH)$), 124.7 (Ar(*C*H) OC_5H_9), 125.3 ($Ar_{calix}(CH)$), 132.2, 132.3, 135.6 (Ar(*C*)CH_2Ar, Ar(*C*)CH_2OAr), 143.8, 144.3 (Ar(*C*)$C(CH_3)_3$), 152.3, 152.8 (Ar(*C*)OPr, Ar(*C*)OCH_2Ar), 153.7 (Ar(*C*)OC_5H_9), 154.7 (Ar(*C*)OPr); the resonances assigned to several quaternary carbons, in particular those of (Ar(*C*)-*C*≡*C*-(*C*)Ar), should be taken with reserve since the corresponding signals are too weak. Anal. calcd. for $C_{114}H_{152}IO_8(C_{134}H_{176}O_{10})_6C_{134}H_{176}IO_{10}$ (degree of polymerization (DP)=8, based on NMR end-group analysis): C, 81.35; H, 8.98%; found: C, 79.99; H, 9.27%. GPC data (THF solution at 35ºC against polystyrene standards): M_n=15660 gmol^{-1}; M_w/M_n=2.09; DP = 8, based on M_n.

Poly((2,5-bis-(*p-t*-butyl-phenoxymethyl)-*p*-phenylene)ethynylene-*alt*-(2,5-bis-2-(*S*)-methylbutoxy-*p*-phenylene)ethynylene (**P2**) was obtained by an identical procedure, using a solution of **2** (50.0 mg, 76.41 µmol) in dry toluene (3.06 mL) and freshly distilled NEt_3 (3.06 mL), $PdCl_2(PPh_3)_2$ (3.75 mg, 5.35 µmol), CuI (1.02 mg, 5.35 µmol), and a solution of **3** (25.04 mg, 83.91 µmol) in toluene. After 24h stirring at 35ºC (degree of conversion *ca.* 94% based on **2**), the workup led to an yellow-orangish solid in 66.9% (35.6 mg); FTIR (ν /cm^{-1} (film)): 3040, 2963, 2931, 2875, 2207 (w), 2147 (vw), 1609, 1513, 1464, 1426, 1385, 1364, 1296, 1276, 1244, 1218, 1186, 1040, 828, 759; UV-Vis (λ_{max}/nm (ε_{max} x 10^{-4} M^{-1}cm^{-1})): 327 (2.375), 435 (5.273);^1H NMR (δ /ppm; $CDCl_3$, 400 MHz): 0.81-0.91 (m, 6H, $-OCH_2CH(CH_3)CH_2CH_3$),

0.93-1.00 (m, 6H, -$OCH_2CH(CH_3)CH_2CH_3$), 1.14-1.40 (m, 20H, -$C(CH_3)_3$ (18H) and -$OCH_2CH(CH_3)CHHCH_3$ (2H)), 1.42-1.78 (m, 2H, -$OCH_2CH(CH_3)CHHCH_3$), 1.77-1.97 (m, 2H, -$OCH_2CH(CH_3)CH_2CH_3$), 3.66-3.80 (m, 2H, -$OCHHCH(CH_3)CH_2CH_3$), 3.81-3.91 (m, 2H, -$OCHHCH(CH_3)CH_2CH_3$), 5.00, 5.31, 5.37 (s, 4H, ArCH_2OAr; *ortho*-CH_2-ArI (chain ends), *meta*-CH_2-ArI (chain ends), -CH_2-Ar (middle chain), respectively; ratio ~1:1:2;), 6.89-7.01 (m, 6H, Ar*H* (*t*-butyl) (4H) and Ar*H*(OC_5H_{11}) (2H)), 7.27-7.36 (m, 4H, Ar*H* (*t*-butyl)), 7.69, 7.77, 8.08 (s, 2H, Ar*H*(CH_2OAr); *meta-H*-ArI (chain ends), Ar*H* (middle chain) and *ortho-H*-ArI (chain ends), respectively; ratio ~1:2:1); ^{13}C NMR (δ /ppm; $CDCl_3$, 100 MHz): 11.2 (-$OCH_2CH(CH_3)CH_2CH_3$), 16.6 (-$OCH_2CH(CH_3)CH_2CH_3$), 26.1 (-$OCH_2CH(CH_3)CH_2CH_3$), 31.5 (-$C(CH_3)_3$), 34.1 (-$C(CH_3)_3$), 34.7 (-$OCH_2CH(CH_3)CH_2CH_3$), 67.9 (ArCH_2OAr), 74.2 (-$OCH_2CH(CH_3)CH_2CH_3$), 92.1, 99.6 (-C≡C-), 114.5 (Ar(*C*H)OCH_2Ar), 116.8, 117.5 (Ar(*C*)C≡C-), 126.3 (Ar(*C*H)$C(CH_3)_3$), 126.4 (Ar(*C*H)OAlkyl), 130.1 (Ar(*C*H)CH_2OAr), 138.5 (Ar(*C*)CH_2OAr), 143.7 (Ar(*C*)$C(CH_3)_3$), 153.6, 156.4 (Ar(*C*)OAlkyl, Ar(*C*)OCH_2Ar). Anal. calcd. for $C_{28}H_{32}IO_2(C_{48}H_{56}O_4)_2C_{48}H_{56}IO_4$ (DP=4, based on NMR end-group analysis): C, 75.25; H, 7.34%; found: C, 75.65; H, 7.65%. GPC data (THF solution at 35ºC against polystyrene standards): M_n=5945 gmol^{-1}; M_w/M_n=1.94; DP = 8, based on M_n.

Results and discussion

Synthesis, structural characterization, and photophysical properties. The syntheses of the target polymers, **P1** and **P2**, were carried out as outlined in Scheme 1 and described in the Experimental Section, closely following our previously reported procedures.[9a] The common participating comonomer, 1,4-diethynyl-2,5-bis((*S*)-2-methylbutoxy)benzene (**3**), was prepared from 2,5-diiodo-1,4-hydroquinone in three steps (Scheme S1). The other comonomers, diiodo-biscalix[4]arene (**1**) and diiodo-TBP (**2**), were prepared by our reported methods.[7a]

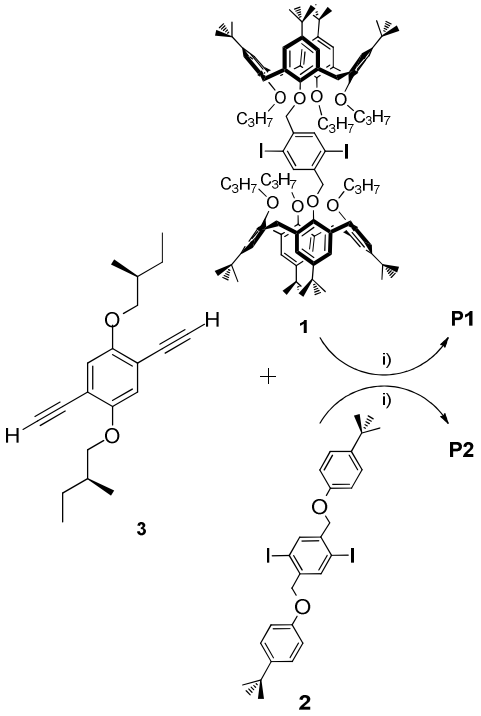

Scheme 1. Synthesis of **P1** and **P2** copolymers: i) $PdCl_2(PPh_3)_2$ (7 mol%) and CuI (7 mol%) in triethylamine/toluene, 35ºC, 24h.

Sonogashira-Hagihara-type cross-coupling copolymerisations of **1** and **2** with diethynyl **3** were performed using Pd(II)/Cu(I) catalysts and proceeded with conversions of 97% and 94% for **1** and **2**, respectively. The crude polymers were purified by dissolution/precipitation sequences until the residual monomer content was less than *ca*. 1.0%, affording **P1** and **P2** in good isolated yields (65 and 67%, respectively).

^{1}H and ^{13}C NMR analysis are entirely consistent with the proposed structures (details of NMR assignments based on COSY, NOESY, HSQC and HMBC techniques may be found in the Experimental Section; spectra in Electronic Supplementary Information (ESI)). No terminal ethynylic C≡C-H protons were found in the ^{1}H NMR spectra of both polymers, indicating that each polymer chain is end-terminated by aryl iodide functionalities. These results fully agree with FTIR data (absence of -C≡*C-H* and *C*≡*C*-H stretching vibrations). The M_n of the polymers

was calculated by ^{1}H NMR end-group analysis and GPC. For **P1** the aromatic signals appearing as multiplets at 7.78, 7.98, and 8.32 ppm (*ca*. 1:6:1 integral ratio), assigned to terminal *meta*-H-ArI, middle chain H-Ar(-C≡C-)$_2$-H, and terminal *ortho*-H-ArI, respectively, were used for the calculation, resulting in an M_n of 15532 gmol^{-1} (DP=8). For the model polymer, the calculated M_n is 2745 gmol^{-1} (DP=4). GPC traces show monomodal distributions for both polymers. The estimated DP of **P1** based on GPC data agrees reasonable well with that retrieved from NMR, while for **P2** the DP seems to be overestimated by GPC (DP ~ 8). This is a known fact for simple rigid-rod-type oligomers and polymers (eg. *p*-phenylene ethynylene and thiophene ethynylene type) where the calculated M_n based on polystyrene standards (which are randomly coiled) are normally well above (by a factor of 1.4-3) their actual molecular weights.[1a,21]

A greater solubility in non-protic organic solvents (THF, CH_2Cl_2, $CHCl_3$, hexane and toluene) was noticed for **P1** in comparison to the model.

The absorption and steady-state fluorescence spectra of **P1** and **P2** in solution and in thin films are shown in Figure 2.

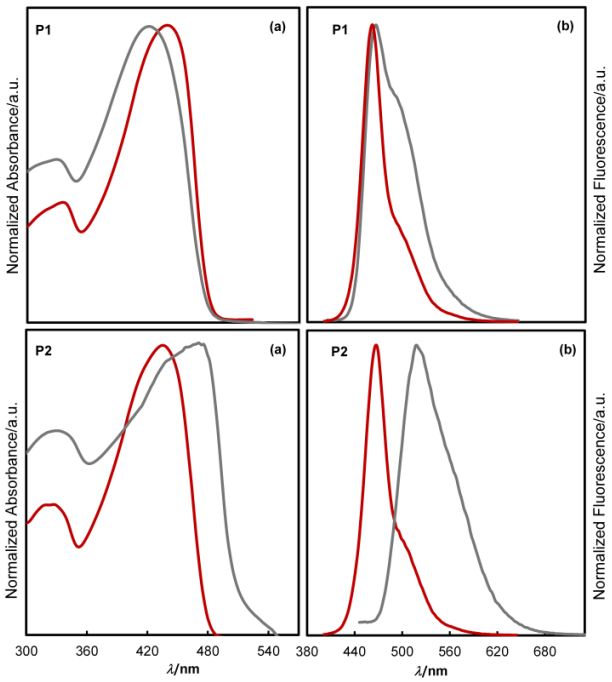

Figure 2. Absorption (a) and emission (b) spectra of **P1** and of **P2** in solution (orange) and in thin film (gray). Excitation at 380 nm (RA and FF geometries for liquid and solid-state, respectively).

The polymers display nearly identical absorption and emission spectra in solution. The fluorescence spectra are characterized by emission maxima at 462-467 nm with shoulders due to vibronic progressions around 500 nm, which are typical features of PPEs possessing alkoxy side-chains.[3] **P1**, in addition to its very high fluorescence quantum yield (unity) in chloroform solution, shows a remarkable photostability. Indeed, under conditions of continuous irradiation (λ_{exc} = 380 nm, air-equilibrated $CHCl_3$ solutions) no noticeable photobleaching or photodegradation occur up to 1h exposure.

Drop-casted films of both polymers prepared from $CHCl_3$ solutions (2.5 x 10^{-3} M) revealed striking different features in their ground-state and, particularly, excited-state spectra. The ground-state absorption spectrum of **P1** displays a shape quite similar to that obtained in solution, denoting, however, a blue shift (18 nm) of the absorption maximum peaking at 416

nm (Figure 2a; **P1**). Conversely, the absorption spectrum of **P2** is characterized by the emergence of a new maximum at longer wavelength (475 nm) (Figure 2a; **P2**). For the calixarene-based polymer the observed hypsochromic shift may be occasioned by the adoption of a less planar conformation of the polymer backbone, favoured by the bulky side-groups. On the other hand, electronic ground-state interchain interactions between the phenyleneethynylene chromophores and/or their enhanced planarization may account for the observed new band in the aggregated state of the model polymer.[2a]

The solid-state emission spectrum of **P1** resembles that of the fluid phase showing a very small red shift (4 nm) at its 0-0 transition (maximum at 466 nm), and the same vibronic shoulder at *ca*. 500 nm (Figure 2b; **P1**), with the ratio of 0-1/0-0 emission intensities substantially increased due to reabsorption effects in this optically dense conditions.[22] In clear contrast, **P2** exhibits a broad, less-structured emission band at 518 nm (with a perceptible shoulder at ~564 nm), representing a red shift of *ca*. 50 nm in the main emission in comparison to solution phase (Figure 2b; **P2**). These low-energy transitions are likely originated from excimeric-states derived from π^*/π intermolecular interactions of phenyleneethynylene units of the backbone,[3,23] and/or from the emission from low-energy states after exciton migration.[11,13c,24]

The most significant photophysical properties of the materials are collected in Table 1.

Table 1. Photophysical properties of **P1** and **P2**.

Polymer	$\lambda_{max,\,abs}$/nm (ε_{max} x10^{-4} M^{-1} cm^{-1}), $CHCl_3$[a]	$\lambda_{max,\,abs}$/nm, film[b]	$\lambda_{max,\,em}$ /nm, $CHCl_3$	$\lambda_{max,\,em}$ /nm, film[b]	Stokes shift/nm[c]	E_g/eV[d]	Φ_F[e]
P1	434 (4.90)	417	462	466	28	2.63	1.00
P2	435 (5.27)	475 (sh 440)	467	518	32	2.59	0.79

[a] Measured at a concentration of 2.0 x 10^{-5} M. [b] Films prepared by drop-coating from 2.5 x 10^{-3} M solutions in $CHCl_3$. [c] The Stokes shifts were calculated from $\lambda_{max,\,em}$ - $\lambda_{max,\,abs}$ in $CHCl_3$. [d] The optical energy gaps (E_g) were calculated from the low energy onset of the absorption bands in $CHCl_3$. [e] Fluorescence quantum yields were determined in $CHCl_3$ using 9,10-DPA as reference (Φ_F= 0.95, in ethanol)[18] at 25ºC; samples and reference excited at 380 nm.

Chiroptical studies in solution and solid state. The chiroptical properties of **P1** and its model **P2** were evaluated by electronic circular dichroism spectroscopy in solution and in the solid state. In chloroform solution (2.0×10^{-5} M), no CD activity was detected at all in the π-π^* transition region (Figure 3a). Keeping the same concentration, gradual addition of methanol (a non-solvent for the polymer) induces the appearance of a CD spectrum which starts to emerge at 35% (v/v) of methanol in the mixture, and reaches its maximum intensity at 55% MeOH (roughly corresponding to the solubility limit of **P1**). The aggregate CD spectrum is dominated by a negative Cotton effect peaking at *ca*. 460 nm, whose maximum has $\Delta\varepsilon$ = -54.5 $M^{-1}cm^{-1}$ at 55% MeOH. The main negative peak has a shoulder on its short-wavelength side, and it is flanked by two smaller positive peaks. Correspondingly, the evolution of the UV-Vis spectra upon addition of methanol is much less marked than CD (Figure 3b). After the addition of 40% methanol, the absorption band becomes only slightly more structured. As discussed in the Introduction, strong interchain interactions are hampered for **P1** by the presence of bis-calixarene units wrapping the backbone, which prevent efficient π-stacking of neighbouring chains. The origin of the observed chiroptical activity of the aggregates may be rationalized as a combination of both *intrachain* (or intrinsic) and *interchain* effects. Among the former ones, the adoption of an induced helix-sense by the polymer main chain is probably the leading source of chiroptical activity.[14c,25] The most important *interchain* effect is the exciton coupling between the strongly dipole-allowed π-π^* transitions of the aromatic backbone.[13c,13e] It must be noticed that exciton coupling is a through-space mechanism which can extend over large distances[26] and is likely to occur at some extent even in loose chromophoric aggregates. A useful quantity to discern the origin of optical activity is the dissymmetry factor ($g_{abs}=\Delta\varepsilon/\varepsilon$).[27] For the main aggregate CD band of **P1**, a moderately large g_{abs}-value (-1.4×10^{-3}) is observed already at 40% MeOH, which is only slightly increased by further methanol addition (-1.8×10^{-3} at 55% MeOH). This value is

almost half-way between those reported for chiral PPEs whose CD spectra have been rationalized as due to solely intrachain[25b] or mostly interchain[13e] effects, respectively.

The decrease in fluorescence intensity in PE-type polymers due to the formation of aggregate species in solvent/non-solvent mixtures is a general reported phenomenon,[13c,13e,14d] because the establishment of ordered phases tends to favour radiationless decays.[28] Noteworthy, at 40% MeOH, the photoluminescence of **P1** is preserved at *ca*. 50% of its initial intensity (integral ratio in the range 400-650 nm, Figure 3c). The residual quantum yield of Φ_F = 50%, together with the relatively high g_{abs}-values, demonstrates that the supramolecular assembly remains highly emissive in conjugation with a strong induction of chirality (helicity). Further quenching occurs on going up to 55% MeOH where *ca*. 35% of the initial emission remains. As discussed in the Introduction, the preservation of a large fraction of photoluminescence for **P1** is related to the co-existence of bulky and chiral substituents on the polymer skeleton, which both prevent an efficient alignment of the polymer chains.

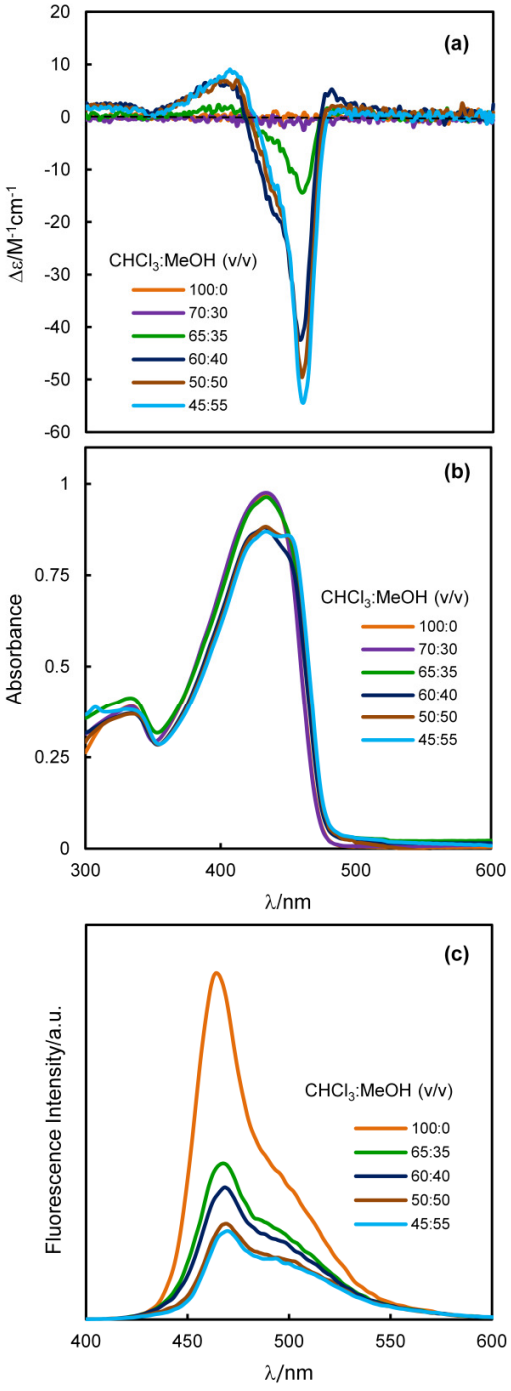

Figure 3. CD (a), UV-Vis (b) and fluorescence (c) spectra of **P1** (2.0×10^{-5}M) in $CHCl_3$:MeOH mixtures. Excitation at 380 nm.

Similar solvatochromic experiments were undertaken for the model polymer **P2**. CD activity starts to be observed at 40% MeOH in the solvent mixture (Figure 4a). In these conditions a positive monosignate Cotton effect appears at 481 nm ($\Delta\varepsilon$ = +18.0 $M^{-1}cm^{-1}$), followed by a weak negative peak around 420 nm. When the methanol content is raised to 50%, significantly different UV-Vis and CD spectra come out. In the UV-Vis spectrum (Figure 4b) an aggregate band appears at 478 nm first as a shoulder and then as a clear band.

In correspondence with this aggregate band, a very intense positive bisignate Cotton effect is observed centred at *ca*. 490 nm. It consists of a peak at 501 nm ($\Delta\varepsilon$ = +63.6 $M^{-1}cm^{-1}$) and a trough at 478 nm ($\Delta\varepsilon$ = -138.4 $M^{-1}cm^{-1}$), with a positive peak-to-trough amplitude of 202 $M^{-1}cm^{-1}$ at 60% MeOH. This strong positive couplet (g_{abs}-value = -4.6 x 10^{-3} at 478 nm) is related to *interchain* exciton coupling between phenyleneethynylene chromophores.[13e] For the model polymer **P2** interchain effects are expected to be dominant over intrachain ones because of a more efficient packing of the polymer chains with respect to **P1**.

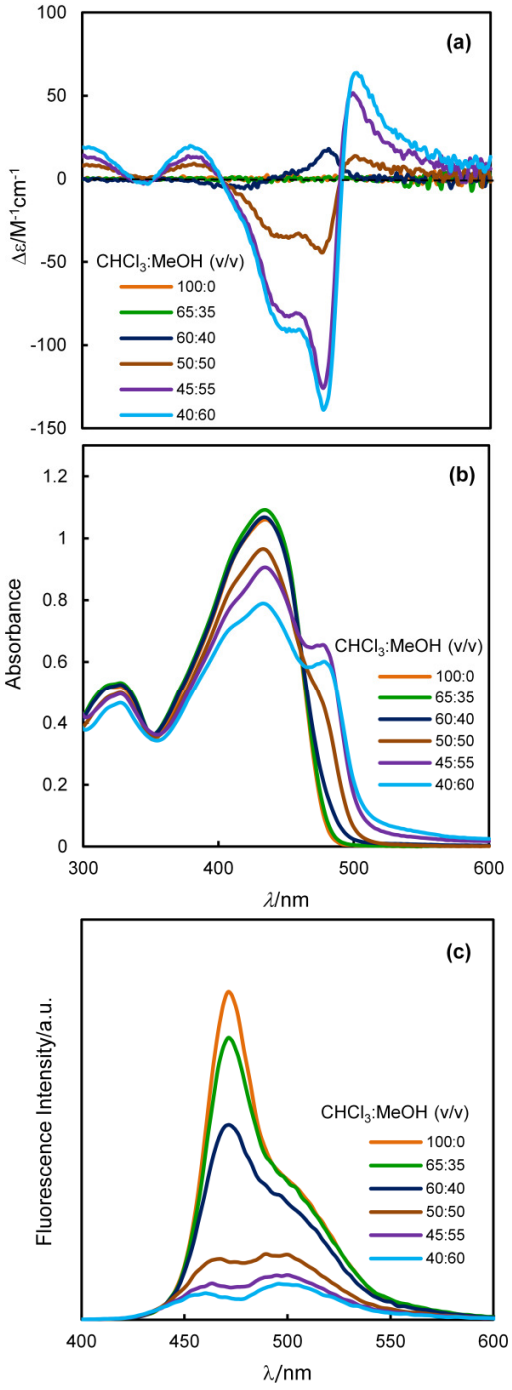

Figure 4. CD (a), UV-Vis (b) and fluorescence (c) spectra of **P2** (2.0×10^{-5}M) in $CHCl_3$:MeOH mixtures. Excitation at 380 nm.

The impact of the polymer aggregation on the fluorescence of **P2** is shown in Figure 4c. At the two methanol-rich mixtures responsible for the highest induced CD signals (55% and 60% MeOH), a marked fluorescence quenching occurs, dropping to less than 20% (integral ratio in the range 400-650 nm) of its initial value, which reduces the quantum yield to Φ_F = 16%. While **P1** retains a similar shape of the emission spectrum upon methanol addition, for the model **P2** the long-wavelength emission band becomes relatively more intense upon aggregation. This band may be attributed to the emission from aggregated species, which is largely but not completely quenched, and originates from red-shifted emissive exciton traps.[11]

The shape of the solid-state (thin films) CD spectra of **P1** and **P2** resemble those of the corresponding solutions (Figure S1), with minor wavelength shifts. We note that the values of the anisotropy factors attained for the drop-casted films are highly dependent on the film preparation, thus precluding any useful quantitative studies, at least with the film-forming technique used here. Nonetheless, g_{abs}-values were consistently lower than those obtained in fluid phase.

Variable temperature experiments. The chiroptical activity and fluorescence of **P1** and **P2** were further examined under a variable temperature regime (-10ºC to 60ºC). The solvent mixtures showing significant CD activities were chosen for the study ($CHCl_3$:MeOH mixtures of 60:40 and 40:60 were used for **P1** and **P2**, respectively).

In both cases, aggregation phenomena were exalted by lowering the temperature from 20° to -10°C (Figures S2 and S3), and were then progressively disrupted by increasing the temperature from -10°C to 60°C (Figures 5 and 6), as expected.

On cooling the solution of **P1** from 20ºC to -10ºC, in fact, a large increment of $\Delta\varepsilon$ is observed at around 460 nm (Figure S2). When the **P1** solution is heated from -10ºC to 60°C (heating rate ~18ºC/min), the shape of the CD spectrum is preserved, but the intensity of the Cotton effects progressively decreases over the temperature range (Figure 5) and, at 60ºC, it is

merely residual (10-15% of its original value). Concomitantly, the UV-Vis spectrum (Figure 5b) loses its structured appearance, and a substantial increase in the fluorescence intensity is noted during the heating period (Figure 5c). On cooling back to 20ºC, the original emission intensity is essentially re-established.

The results obtained after subjecting **P2** to similar cooling/heating sequences differ in some way from **P1**. Indeed, when the **P2** solution was cooled from 20ºC to -10ºC only a small increase in the dichroic signal is observed in clear contrast to **P1** (Figure S3). This may result from the fact that **P2** in 60% MeOH is already strongly aggregated at 20ºC. Performing the heating sequence up to 60ºC, the results are otherwise similar to that obtained for **P1**, that is, a gradual decrease of CD activity (Figure 6a), although at 60ºC a larger chiroptical activity is maintained (*ca*. 30%), accompanied by loss of vibrational structure in the UV-Vis spectra (Figure 6b). The fluorescence spectra also reveal that the disaggregation phenomenon is ongoing upon heating as shown by the progressive change of the relative intensities of the two emission bands located at 459 and 498 nm (20ºC) and the overall intensity increase (Figure 6c). Apparently, however, the original level of aggregation is not restored upon cooling back to 20ºC since neither the emission intensity nor the spectrum shape is the same.

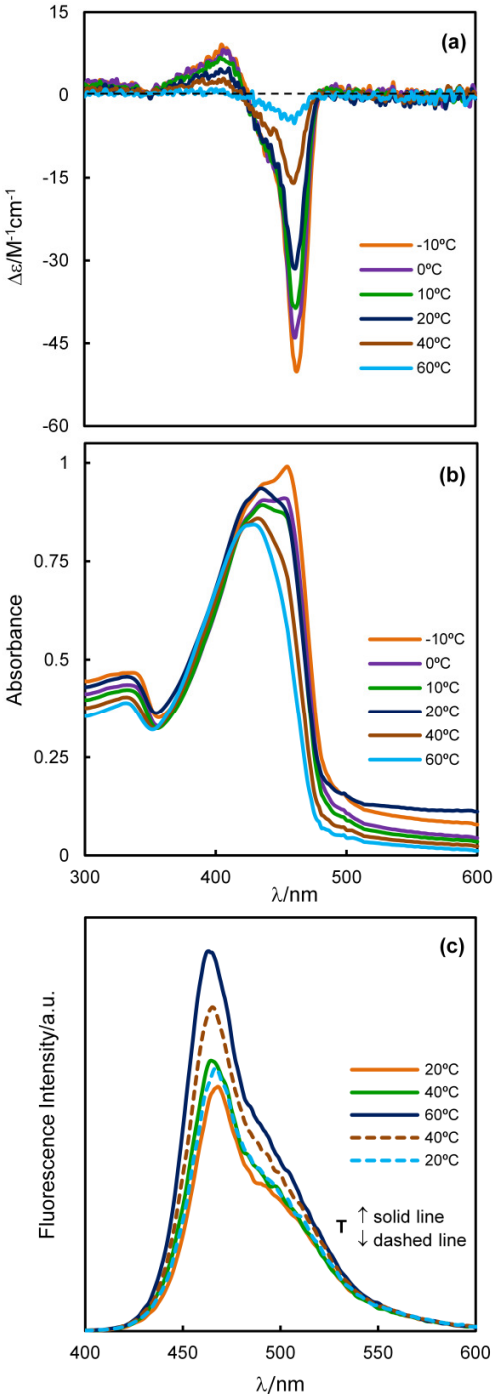

Figure 5. CD (a), UV-Vis (b) and fluorescence (c) spectra of **P1** in $CHCl_3$:MeOH (60:40) mixtures (2.0 x 10^{-5}M) at various temperatures; spectra in (a) and (b) correspond to heating cycles. Excitation at 380 nm.

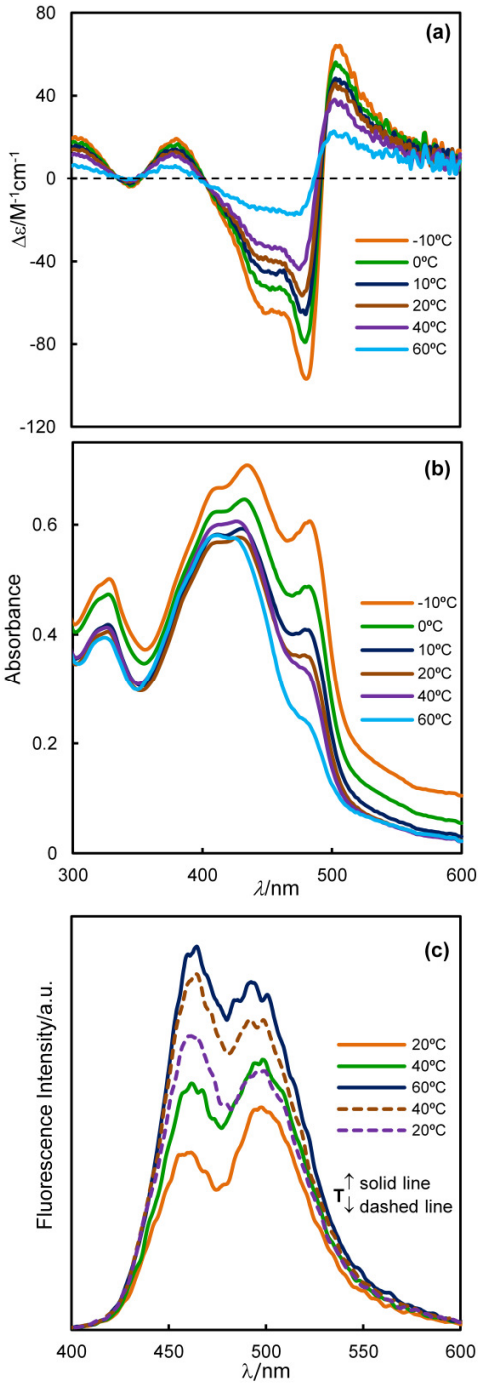

Figure 6. CD (a), UV-Vis (b) and fluorescence (c) spectra of **P2** in $CHCl_3$:MeOH (40:60) mixtures (2.0×10^{-5}M) at various temperatures; spectra in (a) and (b) correspond to heating cycles. Excitation at 380 nm.

The heating/cooling sequence also revealed an unexpected chiroptical behaviour, which was ultimately related to phase separation. In fact, no reversibility in the CD spectrum was found after cooling down the solution of **P1** from 60ºC to 20ºC (cooling rate ~16ºC/min).[29] When the cell was removed from the holder after the heating/cooling cycle, a few dispersed large aggregates could be detected which broke into small particles after shaking. The turbid solution was filtered through a Durapore® membrane (0.45 µm), and the insoluble fraction (IF) re-dissolved in the same solvent mixture. CD and UV-Vis spectra of this fraction (**P1-IF**) and of the filtrate (**P1-SF**) are shown in Figure 7.[30] It is clear that only **P1-IF** displays significant optical activity (g_{abs}-value = -1.3 x 10^{-3} at 464 nm), a result which is also reflected in the absorption spectra (absence of aggregate band in **P1-SF**). Together, the two fractions represent approximately 90% of the total amount of the original sample, with **P1-IF** accounting for *ca*. 55% (estimated from the corresponding ODs at 434 nm). GPC analysis of **P1-IF** and **P1-SF** indicated respectively M_n of 28500 (PDI = 1.69) and 9400 (PDI = 1.50) (Figure S4). When these two fractions were mixed again (**P1**-**M**) and reanalyzed by GPC, the resulting trace was consistent with the original **P1** (a PDI = 2.20 was obtained for the "reconstructed" polymer; Figure S4). The CD spectrum of **P1**-**M** (Figure 7) closely matches the original one taken before the thermal treatment.

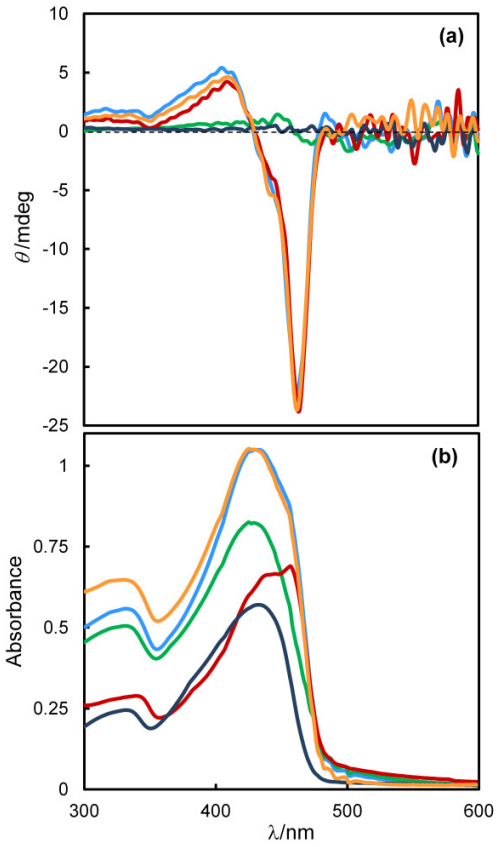

Figure 7. CD (a) and UV-Vis (b) spectra at 20ºC of original **P1** solution (40% MeOH) (blue), **P1** solution after heating to 60ºC (green), **P1-IF** (red) and **P1-SF** (dark blue) processed (see text) after thermal treatment, and **P1**-**M** (orange).

The preceding observations demonstrate that the formation of optically-active solution aggregates of **P1** is achieved only in the presence of high molecular weight polymer chains (number-average DP > 15; $M_{n(GPC)}$= 28500). In other words, the CD activity, and particularly its quantification on a molar basis (*eg.* $\Delta\varepsilon$, g_{abs}-value), depend strongly on the polymer DP. Moreover, the longer polymer chains are involved in thermally-induced aggregation events which lead to the formation of macroscopic particles. The thermal behaviour of **P1** is reminiscent of certain proteins[31a] and synthetic polypeptides[31b] which, on heating, first unfold and then aggregate, following an α-helix-to-β-pleated sheet transition. A similar analysis

performed with **P2** (Figure S5) also established that the observed CD activity is strongly related to the aggregation of polymer chains above a certain critical length (DP_{GPC} ~19; $M_{n(GPC)}$= 13400), despite the differences in the origin of aggregate optical activity discussed above.

Enantiodiscrimination of (*R*)- and (*S*)-α-methylbenzylamine (MBA) by P1 and P2. As a proof of concept of the potential application of polymers **P1** and **P2** as enantioselective sensors, we investigated their binding to the enantiomers of α-methylbenzylamine (MBA). Although CD offers specific advantages in following titration experiments involving chiral species,[16] the non-negligible CD baseline drift observed in the course of time-consuming titrations makes the extractions of binding data less accurate. For that reason, titration experiments were followed by UV-Vis spectral measurements. The titrations were performed by adding increasing amounts of the amines to solutions of **P1** and **P2** in chloroform and in chloroform/methanol mixtures (Figures S6 and S7), at fixed total concentration of 2.0 x·10^{-5} M Monitoring the absorbance changes at 430 nm, a set of binding isotherms were obtained, whereby the association constants (K_a) for the four polymer/amine pairs were calculated by means of a non-linear least-squares method (see ESI for equations and Figures S8 and S9 for curve fittings). In all cases, the binding curves could be fitted on the basis of a 1:1 association model (one molecule of MBA per repeat unit of the polymer). Both **P1** and **P2** displayed small or no tendency to bind MBA when the polymers were in the completely solvated non-aggregated state (chloroform solutions). On the other hand, both polymers in their aggregated state (chloroform/methanol solvent mixtures with at least 40% methanol) bound the enantiomeric amines, although at different extents. In these latter conditions, the calculated association constant for **P1**-(*R*)-MBA [$K_{aP1\text{-}R}$ = (2.5 ± 0.3) x 10^3 M^{-1}] was three times larger than for the **P1**-(*S*)-MBA diastereomeric pair [$K_{aP1\text{-}S}$ = (8.3 ± 2.7) x 10^2 M^{-1}). Thus, **P1** has the capability to discriminate the two enantiomeric amines, and shows a preference for

the (*R*) enantiomer with an enantioselection factor $k_{P1\text{-}R/S} = K_{aP1\text{-}R}/K_{aP1\text{-}S} = 2.7 \pm 1.5$. Conversely, the association constants for **P2** were of similar magnitude for (*R*)- and (*S*)-MBA [$K_{aP2\text{-}R} = (1.7 \pm 0.3) \times 10^3$ M^{-1} and $K_{aP2\text{-}S} = (1.1 \pm 0.2) \times 10^3$ M^{-1}], indicative of a lower discrimination power ($k_{P2\text{-}R/S} = 1.5 \pm 0.5$).

To further extend our knowledge about the stoichiometry of polymer-amine complexes (and also confirm the assumptions made in K_a calculations), the continuous variation method (Job's method) was exploited for the **P1**-(*R*)-MBA pair. The Job plot depicted in Figure S10 (see ESI for details) points to the formation of an *n:n* complex between **P1** and (*R*)-MBA. A 1:1 association[32] was definitely inferred from the data following a recent protocol.[33] This situation corresponds to the binding of one molecule of MBA every two calix[4]arene units, on the average.

Albeit the recognition phenomenon of **P1** toward the chiral amines is not completely understood at this stage, the above results demonstrate that the presence of calix[4]arene units as preferential binding sites is at least as important as the definition of an ordered supramolecular structure. The fact that the chiral discrimination ability of **P1** occurs only in the aggregate state is especially noteworthy. Since solution aggregates are expected to mimic the main features of polymer films, and sensors are normally based on solid materials, the results of our discrimination experiments seem promising in view of potential application of **P1** or similar compounds as enantioselective sensors.

Conclusions

A calixarene-containing chiral aryleneethynylene copolymer (**P1**) and a model chiral polymer devoid of calixarene units (**P2**) were synthesized by a Sonogashira-Hagihara cross-coupling protocol, and their photophysical and chiroptical properties evaluated. The presence of calixarene units and stereodefinite chiral elements along the polymer chain of **P1** prevents

efficient stacking and alignment between polymer chains. This is clearly reflected in their ground-state absorption and steady-state fluorescence, either in solution or in thin films, and is in clear contrast to **P2**. The aggregates of **P1** and **P2** show distinctive chiroptical and fluorescence properties. While in **P1** the chiroptical activity is associated with both intrachain effects (leading to a preferred helical sense of the main chain) and interchain effects (exciton couplings), this latter mechanism is the leading source of chiroptical activity in **P2**. Interestingly enough, it was demonstrated that the formation of optically-active solution aggregates is only achievable above a certain critical molecular weight of the polymer chains. Preliminary studies concerning the enantiorecognition of chiral amines by **P1** and **P2** were undertaken. The results showed that **P1** in its aggregate state is a superior host for (*R*)-α-methylbenzylamine, and a significant enantiodiscrimination between (*R*) and (*S*) amine antipodes was achieved.

The synthetic strategy used lends itself to be easily extended to other structurally differentiated chiral moieties. In that respect, we are planning to exploit chiral natural sources, including various functionalities.

Electronic Supplementary Information (ESI) available: Additional experimental details and data, CD and UV-Vis spectra, GPC traces, titration experiments, Job plot, and NMR spectra. See DOI: ....

Acknowledgements

We thank Fundação para a Ciência e a Tecnologia/MEC (Portugal) for financial support (PEst-OE/EQB/UI0702/2011-2013 and RECI/QEQ-QIN/0189/2012).

Notes and references

1 (a) J. M. Tour, *Chem. Rev.*, 1996, **96**, 537-553; (b) S. Huang and J. M. Tour, *J. Am. Chem. Soc.*, 1999, **121***,* 4908-4909.

2 (a) U. H. F. Bunz, in *Handbook of Conducting Polymers*, 3rd. ed., T. A. Skotheim and J. R. Reynolds, Eds.; CRC Press: New York, 2007; pp 6-1 – 6-51; (b) S. W. Thomas III, G. D. Joly and T. M. Swager, *Chem. Rev.*, 2007, **107**, 1339-1386.

3 U. H. F. Bunz, *Chem. Rev.*, 2000, **100**, 1605-1644.

4 (a) R. A. Bissell, A. P. de Silva, H. Q. N. Gunaratne, P. L. M. Lynch, G. E. M. Maguire and K. R. A. Sandanayake, *Chem. Soc. Rev.*, 1992, **21**, 187-195; (b) A: P. de Silva, H. Q. N. Gunaratne, T. Gunnlaugsson, A. J. M. Huxley, C. P. McCoy, J. T. Rademacher and T. E. Rice, *Chem. Rev.*, 1997, **97**, 1515-1566.

5 D. T. McQuade, A. E. Pullen and T. M. Swager, *Chem. Rev.*, 2000, **100**, 2537-2574.

6 (a) *Calixarenes 2001*; Z. Asfari, V. Böhmer, J. Harrowfield and J. Vicens, Eds.; Kluwer Academic: Dordrecht, 2001; (b) C. D. Gutsche, *Calixarenes: An Introduction*, 2nd ed. In *Monographs in Supramolecular Chemistry*; J. F. Stoddart, Ed.; The Royal Society of Chemistry: Cambridge, 2008.

7 (a) A. I. Costa, L. F. V. Ferreira and J. V. Prata, *J. Polym. Sci. Part A: Polym. Chem.*, 2008, **46**, 6477-6488; (b) P. D. Barata, A. I. Costa, L. F. V. Ferreira and J. V. Prata, *J. Polym. Sci. Part A: Polym. Chem.*, 2010, **48**, 5040-5052; (c) P. D. Barata, A. I. Costa and J. V. Prata, *React. Funct. Polym.*, 2012, **72**, 627-634.

8 J. H. Wosnick and T. M. Swager, *Chem. Commun.,* 2004, 2744-2745.

9 (a) A. I. Costa, H. D. Pinto, L. F. V. Ferreira and J. V. Prata, *Sens. Actuators, B*, 2012, **161**, 702-713; (b) P. D. Barata and J. V. Prata, *ChemPlusChem*, 2014, **79**, 83-89.

10 (a) J. Cornil, D. A. dos Santos, X. Crispin, R. Silbey and J. L. Brédas, *J. Am. Chem. Soc.,* 1998, **120**, 1289-1299; (b) D. Zhao and T. M. Swager, *Macromolecules*, 2005, **38**, 9377-

9384; (c) U. H. F. Bunz, J. M. Imhof, R. K. Bly, C. G. Bangcuyo, L. Rozanski and D. A. V. Bout, *Macromolecules*, 2005, **38**, 5892-5896; (d) F. J. M. Hoeben, P. Jonkheijm, E. W. Meijer and A. P. H. J. Schenning, *Chem. Rev.*, 2005, **105**, 1491-1546.

11 T. L. Andrew and T. M. Swager, *J. Polym. Sci. B*, 2011, **49**, 476–498.

12 For former representative examples, see: (a) J.-S. Yang and T. M. Swager, *J. Am. Chem. Soc.,* 1998, **120**, 5321-5322; (b) M. D. McGehee and A. J. Heeger, *Adv. Mater.*, 2000, **12**, 1655-1668; (c) J. Kim, I. A. Levitsky, D. T. McQuade and T. M. Swager, *J. Am. Chem. Soc.*, 2002, **124**, 7710-7718.

13 (a) B. Erdogan, J. N. Wilson and U. H. F. Bunz, *Macromolecules*, 2002, **35**, 7863-7864; (b) F. Babudri, D. Colangiuli, P. A. Di Lorenzo, G. M. Farinola, O. H. Omar and F. Naso, *Chem. Commun.*, 2003, 130-131; (c) F. Babudri, D. Colangiuli, L. Di Bari, G. M. Farinola, O. H. Omar, F. Naso and G. Pescitelli, *Macromolecules*, 2006, **39**, 5206-5212; (d) T. Ogoshi, Y. Takashima, H. Yamaguchi and A. Harada, *Chem. Commun.*, 2006, 3702–3704; (e) G. Pescitelli, O. H. Omar, A. Operamolla, G. M. Farinola and L. Di Bari, *Macromolecules*, 2012, **45**, 9626-9630.

14 (a) R. Fiesel and U. Scherf, *Macromol. Rapid Commun.*, 1998, **19**, 427-431; (b) R. Fiesel, C. E. Halkyard, M. E. Rampey, L. Kloppenburg, S. L. Studer-Martinez, U. Scherf and U. H. F. Bunz, *Macromol. Rapid Commun.*, 1999, **20**, 107-111; (c) J. N. Wilson, W. Steffen, T. G. Mckenzie, G. Lieser, M. Oda, D. Neher and U. H. F. Bunz, *J. Am. Chem.Soc.*, 2002, **124**, 6380-6381; (d) S. Zahn and T. M. Swager, *Angew. Chem. Int. Ed.*, 2002, **41**, 4226-4230.

15 (a) L. A. P. Kane-Maguire and G. G. Wallace, *Chem. Soc. Rev.*, 2010, **39**, 2545-2576. (b) M. Verswyvel and G. Koeckelberghs, *Polym. Chem.*, 2012, **3**, 3203-3216.

16 G. Pescitelli, L. Di Bari and N. Berova, *Chem. Soc. Rev.*, 2014; doi: 10.1039/C4CS00104D

17 L. Pu, *Acta Polymer.*, 1997, **48**, 116-141.

18 J. V. Morris, M. A. Mahaney and J. R. Huber, *J. Phys. Chem.*, 1976, **80**, 969-974.

19 J. R. Lakowicz, *Principles of Fluorescence Spectroscopy*, 3rd ed.; Springer: New York, 2006; pp 54-55.

20 Q. Zhou and T. M. Swager, *J. Am. Chem. Soc.*, 1995, **117**, 7017-7018.

21 (a) V. Francke, T. Mangel and K. Müllen, *Macromolecules*, 1998, **31**, 2447-2453; (b) H. L. Ricks, U. H. Choudry, A. R. Marshall and U. H. F. Bunz, *Macromolecules*, 2003, **36**, 1424-1425.

22 S. Dhami, A. J. De Mello, G. Rumbles, S. M. Bishop, D. Phillips and A. Beeby, *Photochem. Photobiol.*, 1995, **61**, 341-346.

23 (a) H. Li, D. R. Powell, R. K. Hayashi and R. West, *Macromolecules*, 1998, **31**, 52-58; (b) C. E. Halkyard, M. E. Rampey, L. Kloppenburg, S. L. Studer-Martinez and U. H. F. Bunz, *Macromolecules*, 1998, **31**, 8655-8659.

24 (a) I. D. W. Samuel, G. Rumbles, C. J. Collison, S. C. Moratti and A. B. Holmes, *Chem. Phys.*, 1998, **227**, 75-82; (b) C. Shi, K. Yang and Y. Cao, *Synth. Met.*, 2005, **154**, 121-124.

25 (a) M. Oda, H.-G. Nothofer, U. Scherf, V. Sunjic, D. Richter, W. Regenstein and D. Neher, *Macromolecules*, 2002, **35**, 6792-6798; (b) M. Numata, T. Fujisawa, C. Li, S. Haraguchi, M. Ikeda, K. Sakuraia and S. Shinkai, *Supramol. Chem.*, 2007, **19**, 107-113.

26 B. Moore II and J. Autschbach, *ChemistryOpen*, 2012, **1**, 184-194.

27 (a) S. F. Mason, *Molecular Optical Activity and the Chiral discrimination*; Cambridge University Press: Cambridge, UK, 1982; (b) *Circular Dichroism: Principles and Applications*, 2nd ed; N. Berova, K. Nakanishi and R. W. Woody, Eds.; Wiley-VCH: New York, 2000; pp 185-215.

28 (a) M. M. W. Langeveld-Voss, R. A. J. Janssen, M. P. T. Christiaans, S. C. J. Meskers, H. P. J. M. Dekkers and E. W. Meijer, *J. Am. Chem. Soc.*, 1996, **118**, 4908-4909; (b) B. M. W. Langeveld-Voss, E. Peeters, R. A. J. Janssen and E. W. Meijer, *Synth. Met.*, 1997, **84**, 611-614.

29 When this solution of **P1** was evaporated to dryness and redissolved in the same mixture of solvents (40% MeOH), the CD signal at 20ºC has the same shape and nearly the same intensity as before.

30 This experiment was also performed outside the spectrometer chamber at a later stage. Similar results were achieved within the experimental error.

31 (a) A. Dong, S. J. Prestrelski, S. D. Allison and J. F. Carpenter, *J. Pharm. Sci.*, 1995, **84**, 415-424; (b) C. Chen, Z. Wang and Z. Li, *Biomacromolecules*, 2011, **12**, 2859-2863.

32 The calculated value of $\Sigma c/c_{MAX}$ for the P1-(*R*)-MBA complex, using nine data points, is 5.27, a value that matches the predicted theoretical value (5.25) for a 1:1 association.[33]

33 E. J. Olson and P. Bühlmann, *J. Org. Chem.,* 2011, **76**, 8406–8412.